Modeling for Size Reduction of Agglomerates in Nanoparticle Fluidization

Satoru Matsuda and Hiroyuki Hatano
National Institute of Advanced Industrial Science and Technology, 16-1 Onogawa, Tsukuba, 305-8569, Japan

Tomoya Muramoto and Atsushi Tsutsumi
The University of Tokyo, 7-3-1 Hongo Bunkyo-ku, Tokyo, 113-8656, Japan

DOI 10.1002/aic.10258
Published online in Wiley InterScience (www.interscience.wiley.com).

Nanoparticle fluidization was studied in a centrifugal fluidized bed (CenFB) with variable gravitational acceleration (Gg) conditions. Agglomerate size variation in CenFB nanoparticles (7 nm) was examined with G and fluidization time. With increasing fluidization time, the agglomerate size was found to decrease and reach an equilibrium value after several hours. Higher G reduced agglomerate size. To elucidate these phenomena, a comprehensive model was developed based on the energy balance model with respect to energy consumption for disintegration of agglomerates. Experimental results showed good agreement with the proposed model. Effects of high G on agglomerate fluidization are clarified as follows. The critical minimum size of agglomerates, which is the agglomerate size estimated by the force balance model, is reduced by high G. Attainable energy for disintegration of agglomerates is increased, leading to decreased agglomerate size. © 2004 American Institute of Chemical Engineers *AIChE J,* 50: 2763–2771, 2004

Keywords: agglomeration, nanoparticle, ultrafine particle, centrifugal fluidized bed, high G

Introduction

Ultrafine particles, especially nanoparticles, have recently attracted a great deal of attention because of their increasing potential for wide industrial application. Handling and processing technologies of nanoparticles are very important for industrial application of nanoparticles. If nanoparticles can be handled as highly dispersed particles, important potential applications are anticipated for nanoparticles in various fields. For example, use of ultrafine catalysts in reaction systems leads to high reaction efficiency and rates because of the considerably large specific surface area of nanoparticles. However, large interparticle forces of ultrafine particles often cause undesired agglomeration, leading to handling trouble and reduced productivity.

Nanoparticle fluidization is a promising technology for handling and processing in a multitude of applications of nanoparticles. So far, ultrafine particles have been fluidized while forming agglomerates if the gas velocity is increased far above the minimum fluidization velocity of primary particles. Chaouki et al. (1985) found that fine aerogels are smoothly fluidized. They proposed the force balance model, which assumes that the gravitational force acting on an agglomerate equals the adhesion force attributed to a single contact between two adjacent agglomerates. Morooka et al. (1988) studied fluidity of several kinds of submicron particles and reported that all tested submicron particles form agglomerates during fluidization. The energy balance model was proposed for estimating agglomerate size. Iwadate and Horio (1998) developed the force balance model to predict agglomerate size in a bubbling

Current address of T. Muramoto: Ishikawajima-Harima Heavy Industries Co., Ltd., Tokyo, Japan.

fluidized bed of cohesive powder. In their model, the bed expansion force caused by bubbles is assumed to equal the agglomerate-to-agglomerate cohesive rupture force. Their model was validated by experimental data and compared with previous models. Zhou and Li (1999, 2000) proposed the force balance model to estimate agglomerate size for cohesive powders according to analysis of forces acting on an agglomerate. Model validation was carried out with experimental data. Moreover, they discussed effects of parameters on agglomerate size, showing that higher gas velocity and fluid density, lower particle cohesion, and collision between agglomerates are effective for agglomerate size reduction. In our previous work (Matsuda et al., 2001a), fluidization characteristics of nanophotocatalysts (TiO_2, d_p: 7, 20, and 200 nm) were reported in application to photocatalytic NO_x treatment. It was observed that nanoparticles of TiO_2 clustered into a large agglomerate with the size range of 50 μm to 2 mm. The agglomerate surfaces of 7- and 20-nm particles were smooth, whereas those of 200-nm particles were rough because of the strong adhesion forces of particles. Agglomerate size, surface appearance, and strength were affected by primary particle size.

In spite of advantages of nanoparticle fluidization with agglomeration, formation of agglomerates reduces the potential for nanoparticle applications because of the resultant decrease in specific surface area. It is preferable to suppress formation of agglomerates; agglomerate size should be smaller to exploit the potential of nanoparticles. So far, no studies have addressed the effect of gravitational acceleration on nanoparticle fluidization. The adhesion force of nanoparticles is a key force of agglomerate formation; it is also independent of gravitational acceleration. On the other hand, rupture or disintegration forces are thought to be positively affected by gravitational acceleration. Therefore, if rupture or disintegration forces are increased by increasing G, adhesion forces will become relatively smaller, resulting in achievement of a highly dispersive condition of nanoparticles.

A centrifugal fluidized bed (CenFB) is one high G system. Over the last two decades, fluidization characteristics such as bubble motion, entrainment, pressure drop, and so on have been studied in the CenFB by several researchers (Chen, 1987; Chevray et al., 1980; Fan et al., 1985; Kao et al., 1987; Levy et al., 1978; Qian et al., 1999; Takahashi et al., 1984). Applications of CenFB have also been proposed. Pfeffer et al. (1986) applied the CenFB to a diesel engine dust filter. They reported that CenFB can achieve high collection efficiency. Tsutsumi et al. (1994) studied simultaneous reduction of NO_x and soot exhausted from the diesel engine. They found it can be achieved effectively using the CenFB system. Qian et al. (2001) pointed out that Geldart group C particles can shift to group A particles under a centrifugal force. They confirmed experimentally that C particles (7 μm alumina) can fluidize in a rotating fluidized bed operating at a sufficiently high rotating speed to shift them into group A or B. Our previous works (Matsuda et al., 1998, 2001b) examined fundamental characteristics of ultrafine particle fluidization such as bed expansion, agglomeration, and solid mixing. Ultrafine particles were fluidized while forming agglomerates under high G. Agglomerate size observed near the distributor became smaller with increasing G.

This article describes a comprehensive model of agglomerates in fluidized beds of nanoparticles. An experimental approach using a centrifugal fluidized bed is conducted to validate the proposed model and to elucidate the effect of gravitational acceleration on agglomerate size of nanoparticles.

Fluidization of Nanoparticles

It is well known that almost all nanoparticles can be fluidized smoothly while forming agglomerates. Some researchers have reported fluidization phenomena and proposed agglomeration models addressing fine-particle fluidization. Those models are classified broadly into two categories. One is the force balance model, focusing on forces acting on agglomerates in fluidized beds. These forces have relevance to agglomerate size, d_a, and gravitational force, Gg. Another is the energy balance model, which considers the energy required to break an agglomerate. In this section, nanoparticle agglomeration in a fluidized bed is discussed according to precedent achievements.

Force balance in fluidized beds of agglomerates

Table 1 shows forces that are addressed by the force balance models proposed. In these models, gravitational force, bed expansion force, collision force, and drag force are considered as separation force, F_s. On the other hand, van der Waals force attributed to a single contact point between adjacent agglomerates and van der Waals force between agglomerates are addressed as adhesion force, F_a. Moreover, other forces such as liquid bridge force may become prominent according to the ultrafine particle species. In force balance models, separation forces F_s are considered to be counterbalanced with adhesion forces F_a.

Although previous force balance models can show agglomerate size, it is thought that they do not represent actual agglomerate size in the fluidized bed. All forces handled by previous force balance models are external forces acting on an agglomerate. If the separation force is greater than adhesion force ($F_s \geq F_a$), the agglomerate can be fluidized as an individual fluidized particle. On the other hand, if adhesion force is greater than separation force ($F_s < F_a$), the agglomerates cannot be separated. This means that agglomerates cannot be fluidized individually. Therefore, agglomerate size estimated by force balance models is defined as the critical size in which agglomerates can be fluidized as individual particles.

As can be seen in Table 1, separation and adhesion forces are proportional to $d_a^{n1}G^{n2}$ and $d_a^{n3}G^{n4}$, respectively. Then, the fluidization condition can be expressed as

$$c_1 d_a^{n1} G^{n2} \geq c_2 d_a^{n3} G^{n4} \tag{1}$$

where c_1 and c_2 are constants. Thus, Eq. 1 becomes

$$c_1 d_a^{(n1-n3)} \geq c_2 G^{(n4-n2)} \tag{2}$$

According to Table 1, the value of (n1 $-$ n3) always has a positive value. Therefore, agglomerate size calculated by the force balance models is the critical minimum size of agglomerate, d_{acr}, under a certain operating condition. Thus, the force balance model yields a fluidization/defluidization criterion.

To compare the models, the forces in the force balance models are elucidated using the data for TiO_2 (d_p = 7 nm). The parameters in the calculation and the values of forces are listed

Table 1. Forces Acting on an Agglomerate

Force	Expression	Simplified	F_s (separation) or F_a (adhesion)	n1	n2	n3	n4
Gravitational force–buoyancy	$F_g = \frac{\pi}{6}(\rho_a - \rho_f)d_a^3 g$	$F_g \propto d_a^3 \mathrm{G}^1$	F_s	3	1	—	—
Bed expansion force	$F_{\exp} = \frac{\pi D_b \rho_a (-P_s^*) d_a^2 g}{2n_k}$	$F_{\exp} \propto D_b^1 d_a^2 \mathrm{G}^1$	F_s	2	1	—	—
Collision force	$F_c = 0.166\left(\frac{\pi V^6 \rho_a^3}{k^2}\right)^{1/5} d_a^2$	$F_c \propto D_b^{0.6} d_a^2 \mathrm{G}^{0.6}$	F_s	2	0.6	—	—
Drag force	$F_d = C_D\left(\frac{\pi d_a^2}{4\phi}\right)\frac{\rho_f u_r^2}{2}$	$F_d \propto C_D d_a^2 \mathrm{G}^0$	F_s	1–2	0	—	—
Adhesion force attributed to a single contact point	$F_H = \frac{h_w R}{8\pi\delta^2}\left(1 + \frac{h_w}{8\pi^2\delta^3 H_r}\right)$	$F_H \propto d_a^0 \mathrm{G}^0$	F_a	—	—	0	0
Cohesive force between agglomerates (van der Waals F)	$F_{coh} = \frac{H_a d_a}{24\delta^2}$	$F_{coh} \propto d_a^1 \mathrm{G}^0$	F_a			1	0
Liquid bridge force	$F_1 = \pi r_2 \gamma \frac{r_2 - r_1}{r_1} + 2\pi r_2 \gamma$ $F_{1,\max} = \pi d_a \gamma$	$F_{1,\max} \propto d_a^1 \mathrm{G}^0$	F_a	—	—	1	0

in Table 2. The forces acting on an agglomerate are affected by the agglomerate size. The critical minimum size of agglomerate can be estimated by choosing the agglomerate size when a dominant force of separation forces is equal to that of adhesion forces. In this case, the collision force and the cohesive force between agglomerates (van der Waals force between agglomerates) are selected as dominant force, respectively. The value of d_{acr} is 97 μm at normal G (G = 1) and is decreased to 15 μm at high G (G = 100) because of the increase in the collision force.

Size reduction of agglomerates

Agglomerates are formed in the initial stage of fluidization by their own adhesion force. Agglomerates are subsequently disintegrated into smaller ones. When an agglomerate is disintegrated, energy consumption takes place.

Morooka et al. (1988) proposed the energy balance model for agglomerate formation and disintegration. Energy for agglomerate formation is equal to the energy required to break the agglomerate; it can be written as

$$E_{break} = \frac{\pi d_a^2 \delta}{2}\sigma_t \tag{3}$$

where σ_t is the maximum tensile strength and δ is the distance at which van der Waals force is maximized. The value of maximum tensile strength σ_t is estimated by the theory devel-

Table 2. Parameters in Calculation and Values of Forces in Case of Nanoparticle of TiO_2

Given data*	Primary particle size, d_p	7 nm
	Primary particle density, ρ_p	4000 kg/m^3
	Agglomerate density, ρ_a	300 kg/m^3
	Agglomerate voidage, ε_a	0.925
	Lifshitz–van der Waals constant, h_w	0.92×10^{-19} J
	Hamaker constant, H_a	0.39×10^{-19} J
	Distance between agglomerate, δ	4×10^{-10} m
	Asperities of the agglomerate, R	0.1 μm
	Coefficient that characterizes the hardness of agglomerate, H_r	10^8 N/m^2
	Function of Poisson's ratio and Young's modulus of agglomerate, k	3.0×10^{-6} Pa^{-1}
	Dimensionless particle pressure, P_s^*	−0.07
	Bed voidage, ε	0.5
	Fluid density, ρ_f	1.25 kg/m^3
	Fluid viscosity, μ	1.76×10^{-5} Pa s^{-1}
	Column diameter, D_t	0.01 m
	Settled bed height, L_c	0.05 m
	Superficial gas velocity, u_0	0.5 m/s
	Gravitational acceleration, g	9.8 m/s^2
Solution	Gravitational force–buoyancy, F_g	1.4×10^{-9} N
	Bed expansion force, $F_{\exp}$	2.9×10^{-8} N
	Collision force, F_c	9.9×10^{-7} N
	Drag force, F_d	1.0×10^{-8} N
	Adhesion force attributed to a single contact point, F_H	2.7×10^{-9} N
	Cohesive force between agglomerates, F_{coh}	9.9×10^{-7} N
	Critical minimum size of agglomerate, d_{acr}	97 μm

*Minimum fluidization velocity is estimated by Wen and Yu correlation; bubble size is estimated by Mori and Wen correlation.

oped by Rumpf (1970), assuming that forces are transmitted at coordination points of particles forming the agglomerate

$$\sigma_t = \frac{1 - \varepsilon_a}{\varepsilon_a d_p^2} F_H \tag{4}$$

where ε_a is voidage of the agglomerate, d_p is composition particle size of the agglomerate, and F_H is the adhesion force attributed to a single contact point. Here, a primary particle is considered to be the composition particle of the agglomerate. If van der Waals force is dominant for the adhesion force, F_H can be described as (Krupp, 1967)

$$F_H = \frac{h_w R}{8\pi\delta^2}\left(1 + \frac{h_w}{8\pi^2\delta^3 H_r}\right) \tag{5}$$

where h_w is the Lifshitz–van der Waals constant, R is an asperities of the primary particles, and H_r is a coefficient that characterizes the hardness of agglomerate. Although Chaouki et al. (1985) assumed the asperities of the particles R as 0.1 μm, it must be large in the case of nanoparticles. Morooka et al. (1988) treated R as half of the primary particle size. Here, R is assumed as

$$R = \frac{d_p}{m} \tag{6}$$

where m is a parameter that characterize the asperities of the particles. Substituting Eqs. 4, 5, and 6 into Eq. 3 yields

$$E_{break} = \frac{d_a^2 h_w}{16\delta m d_p}\left(\frac{1 - \varepsilon_a}{\varepsilon_a}\right)\left(1 + \frac{h_w}{8\pi^2\delta^3 H_r}\right) \tag{7}$$

Morooka et al. (1988) focused on energy consumption only at the disintegration of a given agglomerate. However, energy consumption for grinding powder should consider the energy required per unit-weight of agglomerate. Although the energy required to break the agglomerate decreases through disintegration, the number of agglomerates is increased, leading to an increase of total energy required per unit-weight of agglomerates. Here, a modification of energy consumption for disintegration of agglomerates is attempted. Energy consumption required for disintegration of agglomerate per unit-weight of agglomerate E_d can be described using the density of agglomerate ρ_a

$$E_d = E_{break}\frac{6}{\pi\rho_a d_a^3} = \frac{3h_w}{8\pi\delta m\rho_a d_p d_a}\left(\frac{1 - \varepsilon_a}{\varepsilon_a}\right)\left(1 + \frac{h_w}{8\pi^2\delta^3 H_r}\right) \tag{8}$$

Substituting ρ_d/ρ_p into $(1 - \varepsilon_a)$ yields

$$E_d = \frac{3h_w}{8\pi\delta m(\rho_p - \rho_a)d_p d_a}\left(1 + \frac{h_w}{8\pi^2\delta^3 H_r}\right) \tag{9}$$

From Eq. 9, it is clear that E_d is increased by the smallness of primary particle d_p, $(\rho_p - \rho_a)$, which is hard consolidation, and agglomerate size d_a.

Model for estimation of agglomerate size in a fluidized bed

Agglomerate size in a fluidized bed is assumed to be determined by the energy balance with respect to energy consumption for disintegration of agglomerates. In the fluidized bed, agglomerates receive energy for disintegration by fluidization phenomena such as attrition, gas stream shearing, and collision among agglomerates. Therefore, it can be considered that size reduction of agglomerates in fluidized beds is a grinding process. Attainable energy for disintegration of agglomerates E_a in the fluidized bed is likely to be affected by operating conditions such as gas velocity and by experimental-apparatus design. Here, the value of E_a is assumed to be proportional to G^n

$$E_a = c_a G^n \tag{10}$$

where c_a is a parameter that depends on the operating conditions and the experimental-apparatus design.

If the value of E_a is larger than the energy required for disintegration of agglomerates E_d, the agglomerate disintegrates into a smaller one. Disintegration of agglomerates takes place until E_a is equivalent to E_d. Therefore, the size of agglomerate d_a can be given as

$$E_a = E_d \tag{11}$$

By substituting Eqs. 9 and 10 into Eq. 11, d_a can be written as

$$d_a = \frac{3h_w}{8\pi\delta m c_a(\rho_p - \rho_a)d_p G^n}\left(1 + \frac{h_w}{8\pi^2\delta^3 H_r}\right) \tag{12}$$

The influence of operating conditions on d_a can be inferred from Eq. 12. For instance, d_a is decreased by an increase of primary particle size d_p. With increasing $(\rho_p - \rho_a)$ (that is, soft formation of agglomerates), d_a is decreased. These facts indicate that agglomerates will be easily disintegrated into small fragments if formation of agglomerates is soft. Furthermore, d_a decreases with increasing G.

Experimental

Apparatus

Figure 1 shows an experimental apparatus of a high G system using a centrifugal fluidized bed (CenFB). Figure 2 shows an outline of the CenFB. The CenFB, made of steel with a cylindrical distributor, has a 500-mm inner diameter and 10-mm width. A 3-mm-thick distributor is made of twisted 100-μm-diameter wires. Side walls of the bed and a plenum chamber are made of transparent acrylic plate to observe fluidization quality of ultrafine particles. Centrifugal force can be controlled by changing the rotating speed ω of the bed. The centrifugal acceleration ratio to gravitational acceleration G is given as

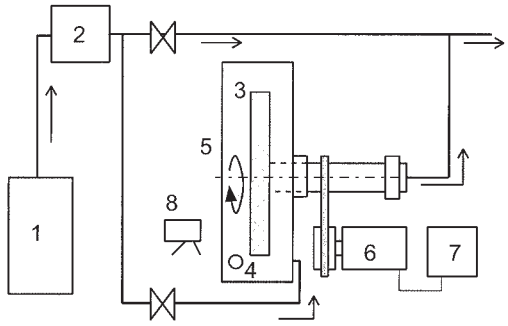

1: Air compressor
2: Mass flow controller
3: Centrifugal fluidized bed
4: Pressure transducer
5: Plenum chamber
6: Motor
7: Motor controller
8: Stroboscope

Figure 1. Experimental apparatus of high G system using a centrifugal fluidized bed.

$$G = \frac{r_o \omega^2}{g} \tag{13}$$

The value of G on the distributor can be regarded as constant throughout the whole bed because of the large radius of the distributor and the shallow bed. The pressure drop is measured by a pressure transducer in the plenum chamber. Rotating speed is measured using a stroboscope.

Ultrafine particles (nanoparticles)

Titanium dioxide (TiO_2) particles, with primary diameter of 7 nm, are used. Tapped bed densities are obtained from the bed volume in each G condition without gas flow and are substituted for agglomerate densities. Figure 3 shows experimental data of tapped bed densities of 7-nm particles. In this case, agglomerate densities ρ_a of 7-nm particles can be defined as constant at 500 kg/m^3 in the range of G from 3 to 100.

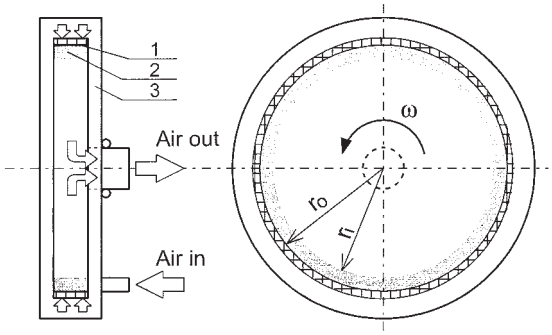

1: Distributor
2: Bed
3: Plenum chamber

r_o : 250 mm
r_i : 200 - 220 mm
ω : 60 - 930 rpm

Figure 2. Outline of centrifugal fluidized bed.

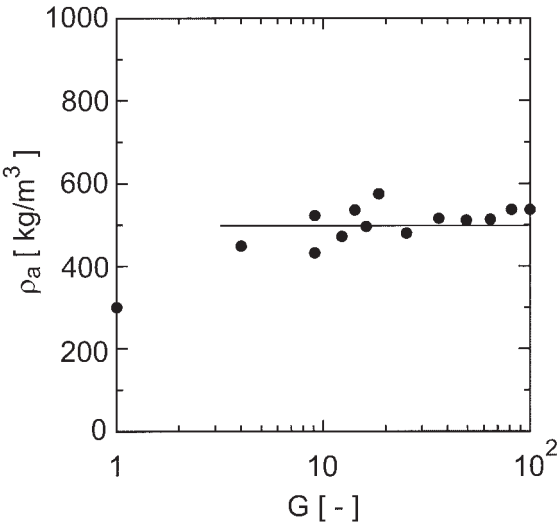

Figure 3. Tapped bed density, substituted for agglomerate density.

Method for experimental estimation of agglomerate size

Agglomerate size in a fluidized bed can be obtained using experimental values of minimum fluidization velocity of agglomerates u_{mf} as reported by Morooka et al. (1988). In high G conditions, it can also be obtained experimentally from u_{mf} values. Minimum fluidization velocity of agglomerates u_{mf} is obtained from the diagram of pressure drop vs. gas velocity and observation of bed expansion. The theoretical u_{mf} for a high G system can be estimated using equations for a conventional fluidized bed (Wen and Yu, 1966), replacing gravitational acceleration g by centrifugal acceleration Gg as follows

$$\mathrm{Ar} = \frac{d_a^3 \rho_f (\rho_a - \rho_f) \mathrm{G} g}{\mu^2} \tag{14}$$

$$\mathrm{Re} = (33.7^2 + 0.0408\ \mathrm{Ar})^{1/2} - 33.7 \tag{15}$$

$$u_{mf} = \frac{\mu\ \mathrm{Re}}{d_a \rho_f} \tag{16}$$

Using experimental data of u_{mf} and ρ_a, agglomerate size d_a can be calculated by simultaneously solving Eqs. 14, 15, and 16.

Procedures

Initially, rotating speed increases at almost 2 G for loading particles onto the circular distributor to form the flat surface of the bed. If an irregular bed surface occurs, the bed is forced to form a flat surface by hand-tapping of the plenum chamber. Subsequently, gas streams are passed into the particulate phase. When bed expansion is observed, the rotating speed is gradually increased until bed expansion is suppressed. Gas velocity and rotating speed are controlled simultaneously until G reaches the desired level. The fluidized bed is kept at a gas velocity of nearly u_{mf} under each G condition. After a stated operation time of fluidization, fluidization examination is conducted for estimation of d_a by measuring u_{mf}. The purpose of the stated operation time is to obtain enough energy for disin-

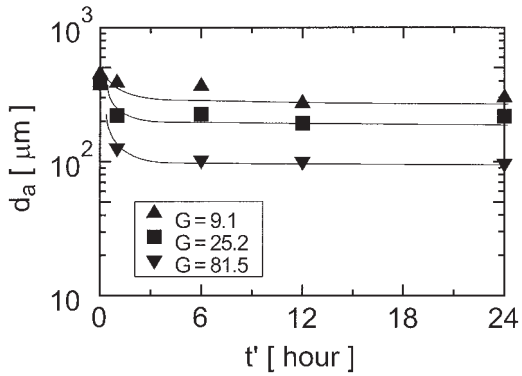

Figure 4. Typical time variation of agglomerate size under high G conditions.

tegration of agglomerates from fluidization phenomena, such as attrition, gas stream shearing, and collision among agglomerates. During fluidization examination for estimation of d_a, the gas velocity is gradually increased. After bed expansion occurs, superficial gas velocity is gradually decreased while measuring the pressure drop of the bed for detection of u_{mf}. Finally, d_a can be obtained from experimental data of u_{mf}.

Results and Discussion

Figure 4 shows typical time variation of agglomerate size under high G conditions. Agglomerate size at the initial stage becomes small in an hour's operation time for all cases. With high G, the agglomerate equilibrium size decreases and operation time to reach equilibrium tends to decrease. It is thought that agglomerates in a fluidized bed of nanoparticles are disintegrated by fluidization phenomena such as attrition, gas stream shearing, and collision among agglomerates, which are positively affected by high G. The attainable energy for disintegration of agglomerates under a certain condition is thought to be constant in this experimental system because agglomerate size reaches equilibrium. Moreover, the requirement of several hours' operation time to reach equilibrium for all cases indicates that the bond in an agglomerate of nanoparticles is thought to be extremely strong compared with that of conventional agglomerates of cohesive powder. In addition, fluidization quality at the initial stage is fairly good from observation of bed expansion and pressure drop of the bed. It can be considered that agglomerate size is larger than the minimum critical size for all cases; also, agglomerate size is determined by energy consumption for disintegration of agglomerates in the fluidized bed.

The typical pressure drop vs. gas velocity diagrams of nanoparticle agglomerate at the equilibrium state are shown in Figure 5. Minimum fluidization velocities of agglomerates u_{mf} are determined from variation in pressure drops decreasing superficial gas velocity. The value of the pressure drop when the gas velocity is larger than u_{mf} is lower than the theoretical values that can be estimated from the initial weight of the bed and the area of the distributor resulting from loss of particles during the experiments. The value of u_{mf} is also confirmed experimentally by observation of bed expansion.

Figure 6 shows agglomerate size d_a evaluated from experimental data of u_{mf} and ρ_a under each G condition. If fluidization

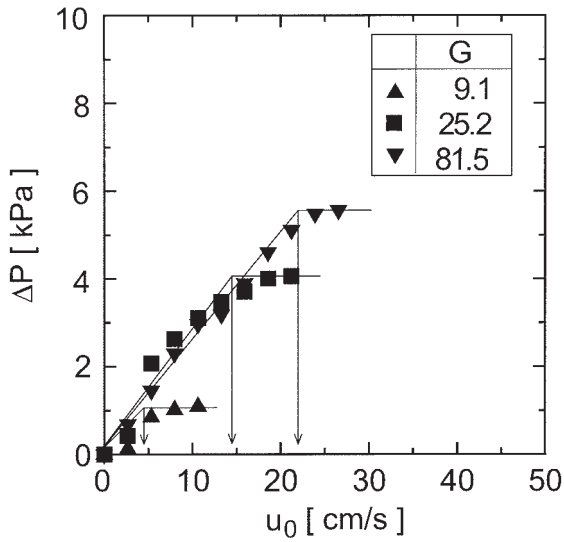

Figure 5. Typical pressure drop vs. gas velocity diagrams under high G conditions after long-time operation.

examination for estimation of d_a is carried out immediately after G reaches the desired value, d_a is observed to decrease slightly with increasing G. On the other hand, d_a is found to decrease to about 100 μm at high G conditions (G = 100) when allowing sufficient time for the fluidization operation near u_{mf}. Thus, agglomerate size d_a decreases under a high G condition with long-time operation, indicating that reduction of agglomerate size consumes energy. Furthermore, agglomerate size reaches a constant value under each G condition, even with a considerably long operation time at a gas velocity of u_{mf}. Morooka et al. (1988) described that the pressure drop of the fluidized bed of fine particles was measured after the bed was fluidized for 30 min. It is considered that they met the transitional state of agglomeration; that is, agglomeration of fine

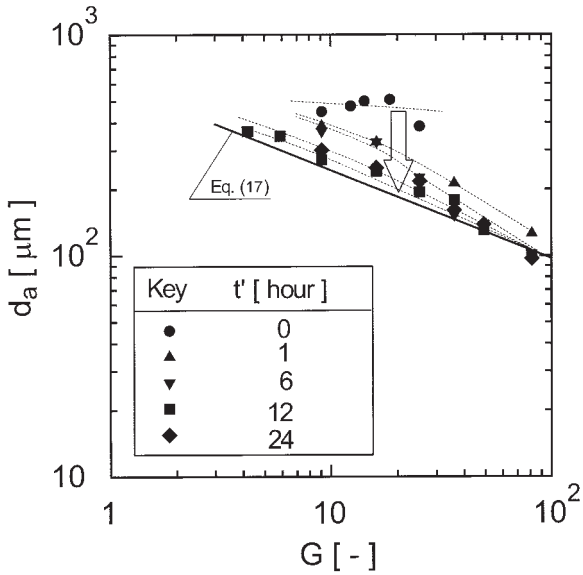

Figure 6. Agglomerate size evaluated from experimental data of u_{mf} and ρ_a under each G condition.

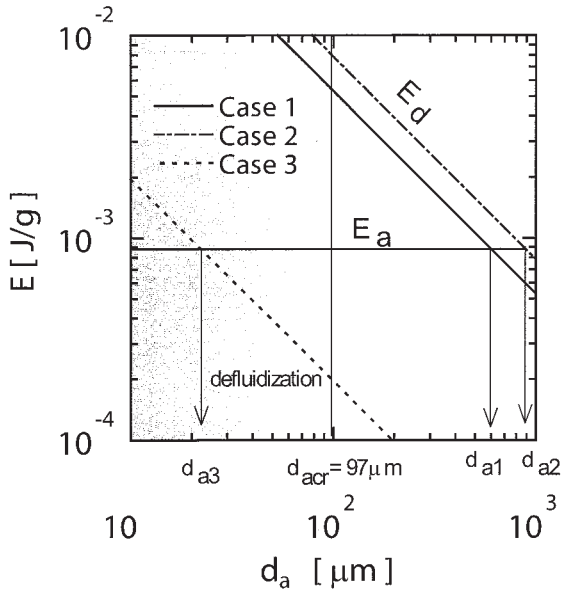

Figure 7. Model for fluidization of agglomerates.

particles was unstable at the beginning fluidization, but it reached an equilibrium state within 30 min.

Using experimental data, equilibrium size of nanoparticle agglomerates in the CenFB system used in this work follows this equation, a modification of Eq. 12

$$d_a = \frac{1.5 \times 10^{-8}}{(\rho_p - \rho_a) d_p G^{0.4}} \tag{17}$$

Schema of the proposed model

Figure 7 shows a diagram for agglomeration of ultrafine particles proposed in this work in a fluidized-bed system. The agglomerate size in a bed can be estimated from the energy balance between E_d and E_a in a fluidized bed. The energy required for disintegration of agglomerates is concerned with agglomerate structure and depends on agglomerate properties such as primary particle (constituent particle) size and agglomerate density. On the other hand, attainable energy for disintegration of agglomerates is thought to be independent of d_a.

Case 1 (TiO_2, d_p = 7 nm). Ultrafine particles form agglomerates using their own interaction forces when the startup of fluidization. Agglomerate size d_{a1} can be estimated from the crossing point between E_a and E_d. If d_{a1} is larger than d_{acr}, it can be estimated by force balance models; agglomerates of d_{a1} can be fluidized.

For example, in the case of TiO_2 (d_p = 7 nm), the agglomerate size estimated by Eq. 17 is 612 μm under normal G. As above mentioned, the critical minimum size of agglomerate d_{acr} is 97 μm in this experimental system (G = 1). Therefore, the agglomerates can be fluidized in this case. At that time, the value of E_d and E_a is 8.6×10^{-4} J/g.

Case 2: Hard Agglomerate (TiO_2, d_p = 5 nm). In contrasting a case of a hard agglomerate with case 1, the energy required for disintegration of the agglomerate is higher than that of case 1, resulting in an increase of the E_d line. Therefore, the agglomerate size in case 2, d_{a2}, estimated from the crossing point between E_d and E_a, becomes higher than d_{a1} of case 1. This case is realized when the primary particle (constituent particle) size decreases and the agglomerate density increases. Moreover, if interparticle forces are increased, such as by adding a binder such as water, the E_d line tends to shift upward. This explains spray granulation in a fluidized-bed system. Agglomerates of d_{a2} ($>d_{a1} > d_{acr}$) can also be fluidized.

When the primary particle size is 5 nm, the value of E_d is increased according to Eq. 9. On the other hand, the value of E_a is equal to that in case 1 when the variables such as operating conditions and experimental-apparatus design are fixed. The agglomerate size d_{a2} becomes 857 μm. The agglomerates can also be fluidized in this case.

Case 3: Soft Agglomerate (TiO_2, d_p = 200 nm). Contrasting the case of a soft agglomerate with case 1, the energy required for agglomerate disintegration becomes lower than that of case 1, resulting in a decrease of the E_d line and agglomerate size d_{a3}. This case can be realized with an increase in primary particle size and a decrease in agglomerate density. If the agglomerate size in case 3, d_{a3}, is smaller than d_{acr}, agglomerates cannot be fluidized because of the large adhesion force among them. Then, the fluidized-bed system forms secondary agglomerates through integration of smaller agglomerates or, alternatively, falls into the defluidization state. In previous works (Matsuda et al., 2001a), the agglomerate size of ultrafine particles (TiO_2, d_p: 7, 20, and 200 nm) was observed using a high-speed video camera. Agglomerate size of 7 nm was larger than that of 20 nm in the same operating condition. Moreover, ultrafine particles of 200 nm were reported to be only slightly fluidized because of interparticle force weakness compared with that of other ultrafine particles of 7 and 20 nm. Morooka et al. (1988) also reported that their $CaCO_3$ particles could not be fluidized smoothly. It is thought that one reason for difficulties in fluidization of these particles is attributable to their weak agglomerate structure (E_d is too small).

When the primary particle size is 200 nm, the value of E_d is decreased according to Eq. 9 and that of E_a is equal to that in case 1. The agglomerate size d_{a3} becomes 21 μm. Because the value of the critical minimum size of agglomerate d_{acr} is 97 μm in this experimental system, the fluidization state will fall into the defluidization state.

Effect of high G

Figure 8 illustrates the effect of G on the present model. The values are calculated in cases of TiO_2 (d_p = 7 nm). The dotted lines and the solid lines indicate the conditions under normal (G = 1) and high (G = 100) G, respectively. The effect of high G on the fluidized bed of ultrafine particle fluidization is as follows. Based on force balance, the critical minimum size d_{acr} tends to become small with increasing G. As mentioned earlier, in the case of 7-nm particles, the values of d_{acr} are 97 and 15 μm at normal (G = 1) and high (G = 100) G, respectively. Therefore, it can be said that the small agglomerates, which cannot be fluidized at normal G, become smoothly fluidized with increasing G.

Energy consumption takes place when agglomerates disintegrate. The energy required for disintegration of agglomerates is increased if agglomerate density is increased. In this experimental system, the agglomerate densities are 300 and 500 kg/m^3 at normal (G = 1) and high (G = 100) G, respectively.

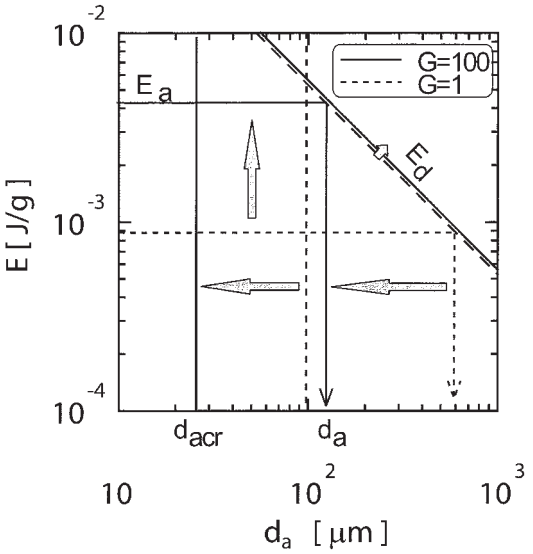

Figure 8. Effect of G on nanoparticle fluidization.

Substituting properties listed in Table 2 and values of agglomerate densities into Eq. 7, the values of E_d can be estimated as follows

$$E_d = \frac{5.3 \times 10^{-7}}{d_a} \qquad (\mathrm{G} = 1) \tag{18}$$

$$E_d = \frac{5.6 \times 10^{-7}}{d_a} \qquad (\mathrm{G} = 100) \tag{19}$$

In this case, the difference between them is negligible. On the other hand, it is thought that attainable energy arises from collisions among agglomerates, shearing by gas streams, and so on. These phenomena seem to be positively affected by high G, resulting in effective reduction of agglomerate size. Using experimental data, the attainable energy can be written as

$$E_a = 8.6 \times 10^{-4}\mathrm{G}^{0.4} \tag{20}$$

by modification of Eq. 10. Therefore, the equilibrium agglomerate size when the value of E_a balances with that of E_d is decreased with increasing G.

Conclusions

A comprehensive model for agglomeration in fluidized beds of nanoparticles was developed based on the energy balance between energy required for disintegration of agglomerates and attainable energy for disintegration of agglomerates. In addition, fluidization/defluidization criteria were shown by the force balance acting on an agglomerate. The experimental approach using a centrifugal fluidized bed was conducted to elucidate the effect of gravitational acceleration on agglomerate size of nanoparticles and to validate the proposed model. It was found experimentally that agglomerate size in a fluidized bed of ultrafine particles decreases as time passes. Agglomerate size is reduced not only with increasing G but also with long-term operation of fluidization. Experimental results showed good agreement with the proposed model. Effects of high G on fluidization of agglomerates were clarified as follows. The agglomerate critical minimum size decreases with high G. Attainable energy for disintegration of agglomerates increases, leading to decreased agglomerate size.

Acknowledgments

This article was presented at the AIChE 2002 Annual Meeting, November 3–8, 2002, Indianapolis, IN. Session "Fundamentals of Fluidization and Fluid Particle Systems."

Notation

Ar = Archimedes number
d_a = agglomerate size, m
c_1 = constant defined by Eq. 1
c_2 = constant defined by Eq. 1
c_a = parameter defined by Eq. 10, J/g
C_D = drag coefficient
D_b = bubble size, m
d_p = primary particle size (constituent particle size), m
E_{break} = energy required to break an agglomerate, J
E_d = energy consumption for disintegration of agglomerate per unit-weight, J/g
E_a = attainable energy for disintegration of agglomerates, J/g
F_a = adhesion force between agglomerates, N
F_c = collision force between agglomerates, N
F_{coh} = cohesive force between agglomerates, N
F_d = drag force, N
F_{exp} = bed expansion force, N
F_g = gravitational force, N
F_H = adhesion force attributed to a single contact point, N
F_s = separation force, N
g = gravitational acceleration, m/s^2
G = acceleration ratio to the gravitational acceleration
H_a = Hamaker constant, J
H_r = coefficient that characterizes the hardness of agglomerate, Pa
h_w = Lifshitz–van der Waals constant, J
k = function of Poisson's ratio and Young's modulus of agglomerate, 1/Pa
m = parameter that characterizes asperities of particles
n = exponent in Eq. 10
n1 = exponent of agglomerate size in separation force (Eq. 2)
n2 = exponent of acceleration ratio in separation force (Eq. 2)
n3 = exponent of agglomerate size in adhesion force (Eq. 2)
n4 = exponent of acceleration ratio in adhesion force (Eq. 2)
n_k = coodinate number of agglomerate
P_s^* = dimensionless particle pressure
R = asperities of particles, m
r_1 = radius of particle, m
r_2 = curvature radius of liquid bridge, m
Re = Reynolds number
r_o = radius of distributor used in centrifugal fluidized bed, m
t' = fluidization time, h
u_{mf} = minimum fluidization velocity, m/s
V = relative velocity of agglomerate, m/s

Greek letters

ϕ = shape factor
γ = surface tension, N/m
ρ_a = agglomerate density, g/m^3
ρ_p = primary particle density, g/m^3
ρ_f = fluid density, g/m^3
μ = fluid viscosity, Pa s^{-1}
δ = distance where van der Waals force is maximum, m
σ_t = maximum tensile strength, Pa
ε_a = agglomerate voidage, —
ω = rotating speed of centrifugal fluidized bed, rad/s

Literature Cited

Chaouki, J., C. Chavarie, D. Klvana, and G. Pajonk, "Effect of Interparticle Forces on the Hydrodynamic Behavior of Fluidized Aerogels," *Powder Technol.*, **43**, 117 (1985).

Chen, Y. M., "Fundamentals of a Centrifugal Fluidized Bed," *AIChE J.*, **33**, 722 (1987).

Chevray, R., Y. I. Chan, and F. B. Hill, "Dynamics of Bubbles and Entrained Particles in the Rotating Fluidized Bed," *AIChE J.*, **26**, 390 (1980).

Fan, L. T., C. C. Chang, Y. S. Yu, T. Takahashi, and Z. Tanaka, "Incipient Fluidization Condition for a Centrifugal Fluidized Bed," *AIChE J.*, **31**, 999 (1985).

Iwadate, Y., and H. Horio, "Prediction of Agglomerate Sizes in Bubbling Fluidized Beds of Group C Powders," *Powder Technol.*, **100**, 223 (1998).

Kao, J., R. Pfeffer, and G. I. Tardos, "On Partial Fluidization in Rotating Fluidized Beds," *AIChE J.*, **33**, 858 (1987).

Krupp, H., "Particle Adhesion, Theory and Experiment," *Adv. Colloid Interface Sci.*, **1**, 111 (1967).

Levy, E., N. Martin, and J. Chen, "Minimum Fluidization and Startup of a Centrifugal Fluidized Bed," *Fluidization*, Cambridge University Press, Cambridge, UK, pp. 71–75 (1978).

Matsuda, S., H. Hatano, and K. Tsuchiya, "Effects of Operating Conditions on Photocatalytic Reduction of NOx in Fluidized Beds of TiO_2," *Fluidization IX*, L.-S. Fan and T. M. Knowlton, eds., Engineering Foundation, New York, pp. 701–708 (1998).

Matsuda, S., H. Hatano, and A. Tsutsumi, "Ultrafine Particle Fluidization and Its Application to Photocatalytic NOx Treatment," *Chem. Eng. J.*, **82**, 183 (2001a).

Matsuda, S., H. Hatano, and A. Tsutsumi, "Particle and Bubble Behavior in Ultrafine Particle Fluidization with High G," *Fluidization X*, M. Kwauk, J. Li, and W.-C. Yang, eds., Engineering Foundation, New York, pp. 501–508 (2001b).

Mori, S., and C. Y. Wen, "Estimation of Bubble Diameter in Gaseous Fluidized Beds," *AIChE J.*, **21**, 109 (1975).

Morooka, S., K. Kusakabe, A. Kobata, and Y. Kato, "Fluidization State of Ultrafine Powders," *J. Chem. Eng. Jpn.*, **21**, 41 (1988).

Pfeffer, R., G. I. Tardos, and E. Gal, "The Use of a Rotating Fluidized Bed as a High Efficiency Dust Filter," *Fluidization V*, K. Ostergaard and A. Sorensen, eds., Engineering Foundation, New York, pp. 667–674 (1986).

Qian, G.-H., I. Bagyi, I. W. Burdick, R. Pfeffer, H. Shaw, and J. G. Stevens, "Gas–Solid Fluidization in a Centrifugal Field," *AIChE J.*, **47**, 1022 (2001).

Qian, G. H., I. Bagyi, R. Pfeffer, H. Shaw, and J. G. Stevens, "Particle Mixing in Rotating Fluidized Beds: Inferences about the Fluidized State," *AIChE J.*, **45**, 1401 (1999).

Rumpf, H., "Zur Theorie der Zugfestigkeit vom Agglomeraten bei Kraftubertragung an Kontaktpunkten," *Chem.-Ing.-Tech*., **42**(8), 538 (1970).

Takahashi, T., Z. Tanaka, A. Itoshima, and L. T. Fan, "Performance of a Rotating Fluidized Bed," *J. Chem. Eng. Jpn.*, **17**, 333 (1984).

Tsutsumi, A., M. Sato, Y. Shibuya, M. Kikuchi, and K. Yoshida, "Simultaneous Removal of Nitrogen Oxides and Soot Emitted from Diesel Engines by a Centrifugal Fluidized Bed," *AIChE Symp. Ser.*, **90**, 152 (1994).

Wen, C. Y., and Y. H. Yu, "A Generalized Method for Predicting the Minimum Fluidization Velocity," *AIChE J.*, **12**, 610 (1966).

Zhou, T., and H. Li, "Estimation of Agglomerate Size for Cohesive Particles During Fluidization," *Powder Technol.*, **101**, 57 (1999).

Zhou, T., and H. Li, "Force Balance Modeling for Agglomerating Fluidization of Cohesive Particles," *Powder Technol.*, **111**, 60 (2000).

Manuscript received Apr. 4, 2003, and revision received Feb. 18, 2004.